BioMACROMOLECULES

Article

pubs.acs.org/Biomac

Poly(carboxylic acid)-Cyclodextrin/Anionic Porphyrin Finished Fabrics as Photosensitizer Releasers for Antimicrobial Photodynamic Therapy

Maria Angela Castriciano,[†] Roberto Zagami,[†] Maria Pia Casaletto,[‡] Bernard Martel,[§] Mariachiara Trapani,[†] Andrea Romeo,[†,∥,○] Valentina Villari,[⊥] Maria Teresa Sciortino,[∥] Laura Grasso,[∥] Salvatore Guglielmino,[∥] Luigi Monsù Scolaro,[†,∥,○] and Antonino Mazzaglia*[,†]

[†]Consiglio Nazionale delle Ricerche, Istituto per lo Studio dei Materiali Nanostrutturati c/o Dipartimento di Scienze Chimiche, Biologiche, Farmaceutiche ed Ambientali, University of Messina, V.le F. Stagno D'Alcontres, 31, 98166, Messina, Italy

[‡]Consiglio Nazionale delle Ricerche, Istituto per lo Studio dei Materiali Nanostrutturati, Via Ugo La Malfa, 153, 90146, Palermo, Italy

[§]Unité Matériaux et Transformations, UMET CNRS 8207, University of Science and Technology of Lille, 59655, Villeneuve d'Ascq, France

[∥]Dipartimento di Scienze Chimiche, Biologiche, Farmaceutiche ed Ambientali, University of Messina, Viale F. Stagno d'Alcontres, 31, 98166, Messina, Italy

[⊥]Consiglio Nazionale delle Ricerche, Istituto per i processi Chimico-Fisici, Viale F. Stagno d'Alcontres 37, 98158, Messina, Italy

[○]C.I.R.C.M.S.B, Unity of Messina, Messina, Italy

Supporting Information

ABSTRACT: In the development of new antibacterial therapeutic approaches to fight multidrug-resistant bacteria, antimicrobial photodynamic therapy (aPDT) represents a well-known alternative to treat local infections caused by different microorganisms. Here we present a polypropylene (PP) fabric finished with citrate-hydroxypropyl-βCD polymer (PP-CD) entrapping the tetra-anionic 5,10,15,20-tetrakis(4-sulfonatophenyl)-21*H*,23*H*-porphine (TPPS) as photosensitizer-eluting scaffold (PP-CD/TPPS) for aPDT. The concept is based on host–guest complexation of porphyrin in the cavities of CDs immobilized on the PP fibers, followed by its sustained and controlled delivery in release medium and simultaneous photoinactivation of microorganisms. Morphology of fabric was characterized by optical (OM) and scanning electron microscopies (SEM). Optical properties were investigated by UV–vis absorption, steady- and time-resolved fluorescence emission spectroscopy. X-ray photoelectron spectroscopy (XPS) and FT-IR revealed the surface chemical composition and the distribution map of the molecular components on the fabric, respectively. Direct $^1O_2$ determination allowed to assess the potential photodynamic activity of the fabric. Release kinetics of TPPS in physiological conditions pointed out the role of the CD cavity to control the TPPS elution. Photoantimicrobial activity of the porphyrin-loaded textile was investigated against both Gram-positive *Staphylococcus aureus* ATCC 29213 (*S. aureus*) and Gram-negative *Pseudomonas aeruginosa* ATCC 27853 (*P. aeruginosa*). Optical microscopy coupled with UV–vis extinction and fluorescence spectra aim to ascertain the uptake of TPPS to *S. aureus* bacterial cells. Finally, PP-CD/TPPS fabric-treated *S. aureus* cells were photokilled of 99.98%. Moreover, low adhesion of *S. aureus* cells on textile was established. Conversely, no photodamage of fabric-treated *P. aeruginosa* cells was observed, together with their satisfying adhesion.

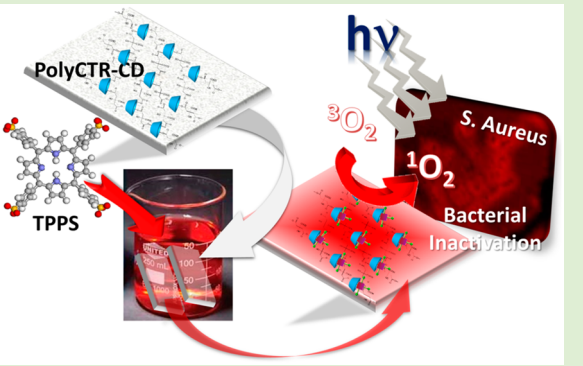

INTRODUCTION

Prevention of infection is a major medical and financial issue. Nowadays, as the increase in multidrug-resistant bacteria, due to the overstated use of antibiotics, research efforts are directing on new antibacterial therapeutic approaches. Antimicrobial Photodynamic Therapy (aPDT) is a well-known alternative to treat local infection caused by different microorganisms, such as Gram-positive and Gram-negative bacteria, viruses, fungi and protozoa.[1,2]

aPDT mechanism involves a photosensitizer (PS), which, released in the infected site, is promoted to its excited singlet state (^{1}PS) by shining light on its absorption bands. This species evolves to the triplet state (^{3}PS) that can decay by transferring energy to the surrounding oxygen and molecular

Received: November 28, 2016
Revised: February 16, 2017
Published: March 3, 2017

DOI: 10.1021/acs.biomac.6b01752
Biomacromolecules XXXX, XXX, XXX–XXX

components. Radical oxygen species (ROS) and, in particular, singlet oxygen ($^1O_2$), are generated and are responsible for the photodynamic damage.[3,4] aPDT is being investigated in the treatment of surface wounds, burns, abscesses, oral sites, and the middle ear infections. While preclinical aPDT studies have largely been carried out by using primarily PS in solution,[3,4] there is an increasing debate to develop photodynamic anti-infective surfaces both with permanent microbicidal activity and with PS releasing properties.[5] According to this approach, PS is generally localized in the implant,[6] and the produced $^1O_2$ plays cytotoxic activity at the required distance in the infected sites, preserving healthy tissues. Recently, Mosinger et al. have proposed different materials based on nanofibers bound to cationic and neutral PSs, clarifying the site of interactions of PS in the polymeric matrix[7,8] and thus controlling the photobactericidal activity.[9,10] PS-conjugate cellulose fibers[11] have been proposed as scalable scaffolds for anti-infective or self-sterilizing materials.[12−14] Furthermore, inorganic nanostructured materials have been employed to modify textile surfaces.[15] When gold nano-objects decorate the surface, they can be activated by suitable light, leading to photothermal destructions of pathogens.[16,17] In this direction, Martel et al. have extensively developed biocompatible cyclodextrin (CD) finished surfaces for controlled drug delivery from vascular eluting stents,[18] textile polyester prosthesis,[19] and polypropylene inguinal meshes.[20,21] The key role of the hydrophobic macrocycle cavity in entrapping and sustaining release of therapeutics to the sickly tissues has been pointed out. Recently, antibacterial surfaces fabricated by embedding antibacterial agents into polyelectrolyte multilayers assembled on supports[22,23] or onto polycationic hydrophobic polymer grafted on glass[24] have been proposed. With this aim in mind, different CD-polymer coatings were designed, that is, by using polyelectrolyte multilayer CD films built-up by the layer-by-layer technique.[25] To this purpose, polycationic polymers, such as chitosan or epichlorohydrin-CD polymer carrying trimethylammonium groups, and polyanionic polymer, such as citric acid-CD polymer,[26,27] have been exploited. Alternatively, reactive groups have been introduced on CD to increase the CD amount grafted on cotton fabrics.[28] One of the main advantages of this approach is the high versatility in the complexation of different typology of drug molecules in natural or modified CD[29−31] or in CD nanogels.[32] Here we present a polypropylene (PP) fabric finished with citric acid-hydroxypropyl-β-CD polymer (PP-CD) entrapping the tetra anionic 5,10,15,20-tetrakis(4-sulfonatophenyl)-21*H*,23*H*-porphyrine (TPPS). TPPS was extensively considered as model compound to investigate the cellular uptake of PS delivered by CD nanoassemblies for PDT.[33] Furthermore, the entrapping of TPPS in CDs is prevalently governed by interaction of the PS with the cavity.[34] Few papers report on photoinactivation of bacteria by both anionic or neutral PS in solution, due to their low interaction with biological membrane.[35,36] On the other hand, a plethora of examples relies on the utilization of cationic PS free in solution or loaded in nanoparticles to photoinactivate Gram-positive or Gram-negative bacterial strains,[3,4,35,37−40] fungi, and viruses.[41] Recently, TPPS and its Ni(II) and Zn(II) metal derivatives have been proposed for photoinactivation of Gram-negative bacteria.[42] aPDT was applied after PS localization in implanted intraocular lens,[6] following cataract surgery, or in wound coverings for the treatment of skin ulcers.[9] But, to the best of our knowledge, rare studies were dedicated to aPDT treatment of nosocomial infection, supplemental to surgery, using photodynamic coverings with sustained release (i.e., after laparoscopic surgery) activated by optical fibers of suitable wavelength.[43] In this direction, here we propose a finished fabric based on host−guest interaction between PP-CD and TPPS for potential application in the fabrication of novel anti-infective implants or coverings. PS entrapped in CD and localized on the covering surface could be efficiently eluted in controlled fashion to neighboring tissues where bacterial cells are nested. As a consequence, bacterial cells (directly in contact with surface or present in the surrounding biological media) could be photoinactivated upon irradiation, preventing bacterial adherence, the first stage of biofilm formation. With respect to aPDT by using PS in solution or entrapped in nanoparticles, the current approach could be suitable to treat postsurgical local infections, thus, minimizing the undesirable photosensitization effect due to the PS systemic administration.[44] Hence, TPPS utilization can be advantageous (i) to minimize dark toxicity, typical of cationic PS, when porphyrin elutes from fabric and enters into in circulation, and (ii) to be released in controlled way from CD cavity where it can plausibly be complexed.[34]

Finished PP-CD/TPPS fabric morphology, chemical composition, and photophysical properties were investigated by complementary microscopic and spectroscopic techniques. Luminescence direct $^1O_2$ determination allowed to evaluate the potential photodynamic activity of the textile.

Finally, photodynamic antimicrobial properties of PP-CD/TPPS fabric were investigated against Gram-positive *Staphylococcus aureus* ATCC 29213 (*S. aureus*) and Gram-negative *Pseudomonas aeruginosa* ATCC 27853 (*P. aeruginosa*), two of the most infective agents associated with medical devices.[45−47]

MATERIALS AND METHODS

Chemicals. Solvents were purified and dried using standard techniques. All the other reagents were of the highest available commercial grade. They were used as received or purified by distillation or recrystallization when necessary. All solutions used for spectroscopic characterizations were prepared in pure microfiltered water (Galenica Senese, Siena, Italy). Hydroxypropyl-βCD (HP-βCD), Kleptose HP, MS = 0.85, where MS is the number of HP groups per glucose units, was purchased from Roquette (Lestrem, France). Citric acid monohydrate (CTR) and sodium dihydrogen hypophosphite (NaH_2PO_2) were purchased from Aldrich chemicals (Saint Quentin Fallavier, France). 5,10,15,20-Tetrakis(4-sulfonatophenyl)-21*H*,23*H*-porphine (TPPS), 5,10,15,20-tetrakis(1-methyl-4-pyridinium)porphyrin (H_2T_4), and 1-adamantanol (Ada-OH) were purchased from Sigma-Aldrich (Milan, Italy).

Preparation of Fabric. PP-CD samples were prepared by a method previously reported.[21] Briefly, PP nonwoven fabric was preliminarily washed by Soxhlet with various solvents (petroleum ether, isopropanol and water) to eliminate industrial finishing products, especially sizing agents. Thereafter, the fabric was treated with a pad−dry process using a horizontal two-roll padder and a thermofixation oven (Roaches, Leek, U.K.). The padding liquor was an aqueous solution containing CTR/NaH_2PO_2/HP-βCD in a 10/3/10 molar ratio, corresponding to the amount in grams of each reactant for 100 mL of solution. Impregnated fabrics were then roll-squeezed, dried, and thermofixed and, finally, washed with hot water by a Soxhlet extractor. Raw and treated samples were dried for 30 min at 104 °C before being weighed. The weight gain of the treated fabric was 15% wt, calculated by the following equation: % wt = $100 \times (m_f - m_i)/m_i$, where m_i and m_f are the weight of the sample before and after treatment, respectively. The precision of the weight gain measurements was ±1.5% wt. By taking into account that the water-soluble cross-linked CD polymer (polyCTR-CD) contains about 50% of HP-βCD, as determined by NMR,[48,49] CD grafted on PP was estimated to

DOI: 10.1021/acs.biomac.6b01752
Biomacromolecules XXXX, XXX, XXX−XXX

be ≅0.506 μmol/cm². PP-CD/TPPS complexes were prepared by dipping different samples (1 cm × 1 cm) of PP-CD into porphyrin aqueous solution (1 mM, V = 3 mL) for 3 h. Afterward, the samples were copiously washed with distilled water to obtain colorless wash waters and eventually dried at 60 °C for 2 h.

Drug Loading Studies. Drug loading (DL) was determined by UV−vis absorption using its molar extinction coefficient at the B-band maximum (ε_{414nm} = 5.33 × 10⁵ M^{-1} cm^{-1})[50] after complete displacement of TPPS by dipping PP-CD/TPPS fabric (1 cm × 1 cm) in a saturated aqueous solution of 1-AdaOH (V = 3 mL). DL was expressed as $W_{Tot(TPPS)}$ (mg/cm²), that is, the total amount of TPPS embedded into a (1 cm × 1 cm) PP-CD sample. DL measurements were carried out in triplicate, and the standard deviation value (±SD) was calculated.

Release Studies. The release profiles of TPPS were evaluated in 10 mM phosphate buffer containing NaCl (137 mM) and KCl (2.7 mM) at pH 7.4 (PBS) and at 37 ± 0.5 °C. TPPS release from PP-CD/TPPS was investigated using ≅1 cm × 1 cm sample plunged in PBS (V = 3 mL), placed into a 1 cm path length quartz cuvette, and gently stirred (200 rpm). The amount of TPPS released in solution was evaluated using its molar extinction coefficient as above-described. For comparison, the elution of TPPS was also evaluated in pure water, in water, and in PBS enriched with 1-AdaOH, respectively. Elution experiments were carried out both at 25 and 37 °C ± 0.5 °C. The release/elution experiments were performed in triplicate, and ±SD was calculated. The eluted/released amount of TPPS at a given time from 1 cm × 1 cm PP-CD/TPPS sample was expressed as $(100 \times W_{TPPS}/W_{Tot(TPPS)})$, where W_{TPPS} is the weight of released amount of TPPS and $W_{Tot(TPPS)}$ is the total amount of TPPS loaded in the analyzed patch.

Affinity binding constant (K_a) was estimated by a simplified procedure by considering the following equilibrium:

$$PP\text{-}CD_{(fabric)} + TPPS_{(solution)} \leftrightarrow PP\text{-}CD/TPPS_{(fabric)} \quad (1)$$

where $PP\text{-}CD_{(fabric)}$ and $PP\text{-}CD/TPPS_{(fabric)}$ indicate the CD content on textile without and finished with TPPS, respectively, and $TPPS_{(solution)}$ is porphyrin species in solution in equilibrium with the species entrapped in the fabric.

From eq 1 it is possible to evaluate affinity constant (K_a) as follows:

$$K_a = a_{PP\text{-}CD/TPPS(fabric)}/a_{TPPS(solution)}a_{PP\text{-}CD(fabric)} \quad (2)$$

where $a_{PP\text{-}CD/TPPS(fabric)}$, $a_{TPPS(solution)}$, and $a_{PP\text{-}CD(fabric)}$ are the activities of PP-CD/TPPS, TPPS, and PP-CD, respectively, and for pure solids, $a_{PP\text{-}CD/TPPS(fabric)}$ and $a_{PP\text{-}CD(fabric)}$, can be considered equal to the unit. a_{TPPS} in diluted solutions is approximately equal to the porphyrin concentration ($[TPPS_{(solution)}]$ = 7.8 μM), which has been determined assuming a nearly complete displacement equilibrium (eq 3) by dipping textile ($PP\text{-}CD/TPPS_{(fabric)}$, 1 cm × 1 cm) in a 1-adamantanol satured solution ($1\text{-}AdaOH_{(solution)}$), thus, forming $PP\text{-}CD/1\text{-}AdaOH_{(fabric)}$ and $TPPS_{(solution)}$.

$$PP\text{-}CD/TPPS_{(fabric)} + 1\text{-}AdaOH_{(solution)} \leftrightarrow PP\text{-}CD/1\text{-}AdaOH_{(fabric)} + TPPS_{(solution)} \quad (3)$$

UV−vis, Fluorescence Emission Spectra, and Microscopy. UV/vis spectra were collected using a Hewlett-Packard mod. 8453 diode array spectrophotometer. Fluorescence emission measurements were performed on a Jobin Yvon-Spex Fluoromax 4 spectrofluorimeter, using time-correlated single-photon counting for time-resolved measurements. The excitation source was a NanoLED at 390 nm. All the spectroscopic measurements were carried out at 25 °C. FEG-SEM and OM measures were performed on the facilities at CNR-ISMN (Monterotondo, Roma). FEG-SEM analysis was carried out by using a high brilliance LEO 1530 apparatus equipped with an INCA 450 energy dispersive X-ray spectrometer (EDS) and a back-scattered electron detector.[51] Microscope images were registered on Leica DMRX and MZ FL III optical microscopes, respectively, equipped with a digital camera, for observation in transmittance, reflection, absorption, and fluorescence. Photogeneration of $^1O_2$ by laser excitation of the PS was monitored by luminescence measurements on 1 cm × 1 cm PP-CD/TPPS patch in a 1 cm path length quartz cell in air, as previously described.[52,53]

XPS. Surface XPS analysis was performed by using a Thermo Scientific ESCALAB 250Xi X-ray photoelectron spectrometer, equipped with a microfocusing X-ray twin-crystal monochromator with a 500 mm Rowland circle. The spectrometer can be used for both imaging and small area XPS, thanks to a two-dimensional detector for imaging and a detector based on channel electron multipliers for spectroscopy when high count rates have to be detected. XPS spectra were acquired by using a standard Al anode as X-ray source (Al K_α radiation, $h\nu$ = 1486.6 eV). The 180° hemispherical energy analyzer operated in the CAE mode at a constant pass energy of 20 eV. XPS data analysis was performed by a nonlinear least-squares curve-fitting program using a properly weighted sum of Lorentzian and Gaussian component curves, after background subtraction according to Sherwood et al.[54]

FTIR. Chemical imaging analyses were performed by a NICOLET iN10 MX Infrared Imaging microscope (ThermoFischer Scientific). Infrared chemical images were collected with a single element detector and aperture set at 50 × 50 μm. Spectra were registered at 8 cm^{-1} resolution and the image size was 250 × 250 μm².

Bacterial Photoinactivation Studies. The antimicrobial activity of PP-CD/TPPS was assessed against *Staphylococcus aureus* ATCC 29213 and *Pseudomonas aeruginosa* ATCC 27853. *S. aureus* and *P. aeruginosa* were stored at −80 °C in glycerol/broth medium (30% v/v) and grown in Tryptic Soy broth and Luria−Bertani broth (LB), respectively, incubating at 37 °C under continuous shaking (180 rpm) for 4−6 h. For antimicrobial activity test, 1 mL of each culture was centrifuged (3700 g, 5 min) and washed three times with 2 mL of sterile PBS. The pellets were then resuspended in sterile PBS to a final density of ∼1 × 10⁸ colony forming units × mL^{-1}(CFU/mL). Bacterial counts were evaluated using standard plating methods. A total of 1 mL of bacterial suspension was incubated in the dark with PP-CD/TPPS and PP-CD patches (1 × 1 cm) at 37 °C for 30 min. After the contact with bacterial suspension, patches were, respectively, transferred into a quartz cuvette (previously decontamined with 70% ethanol for 30 min and washed three times with sterile deionized water) through a sterile needle and placed at 5 cm distance from a cold white light of a 50 W halogen lamp (Osram). The irradiating beam was filtered through a UV filter (Hoya glass type UV-34, cutoff: 340 nm) in order to cut the UV component. A 1 cm cell filled with water was used to remove the IR component. Patches without TPPS (PP-CD) were irradiated for 10, 20, and 30 min, respectively. Each PP-CD/TPPS patch was irradiated for 30 min, and overheating was prevented by ventilation. A light dose of ≅5 J cm^{-2} was estimated. At the same time, patches of PP-CD and PP-CD/TPPS were incubated at room temperature in the dark and used as control without irradiation. Then, all the patches, irradiated and not, were removed and transferred into 1 mL of sterile PBS 0.1% Tween 80 and stirred with a blender for 1 min in order to release bacteria entangled in the patches. The 0.1 mL aliquots of each bacterial suspension were collected and then diluted. Each bacterial resuspension was 1:10 serially diluted (100 μL into 900 μL of sterile PBS) six times, and 100 μL from the undiluted and each diluted sample was plated on agar medium. The plates were incubated overnight in the dark at 37 °C. The survival rate was determined by the ratio of CFU/mL of the irradiated sample versus that of the not irradiated identical sample, coming from the dark control. The minimum detection limit was 100 CFU/well. The experiments were carried out in triplicate. For epifluorescence microscopy imaging, the same above-mentioned procedure was used for the PP-CD/TPPS patches, irradiated or not, that were removed and stained with 10 μL of LIVE/DEAD BacLight. Bacterial Viability Kits (Molecular Probe Thermo Fisher Scientific) were incubated for 15 min in the dark and observed using a Leica DMRE epifluorescence microscope equipped with a Leica DC300F Camera. For each sample, at least five images were acquired by Qwin software.

Extinction and Fluorescence Spectra on Bacterial Cells. An aliquot of bacteria suspension (0.1 mL) was incubated in the dark with PP-CD/TPPS patches at 37 °C for 30 min. Hence, suspension was

DOI: 10.1021/acs.biomac.6b01752
Biomacromolecules XXXX, XXX, XXX−XXX

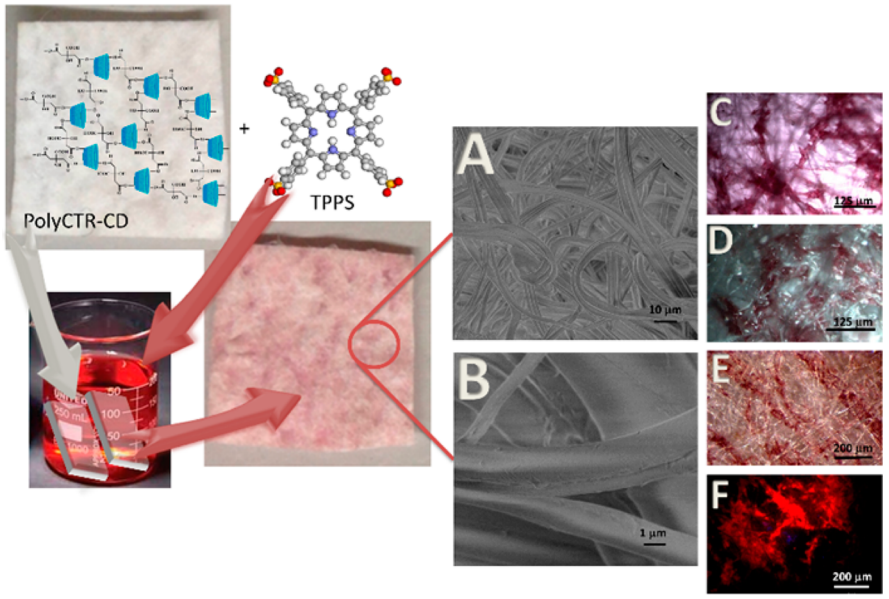

Figure 1. Preparation of fabric based on PP-CD/TPPS with chemical structures of TPPS and PolyCTR-CD coating components and representative FEG-SEM (A, B) and OM images registered in transmittance (C), reflection (D), UV−vis (E), and fluorescence (F) modalities.

centrifuged (3200g, 5 min), washed with 0.5 mL of sterile PBS to eliminate eventual free TPPS, and resuspended in 0.1 mL of fluorescence mounting medium (Agilent Techonologies, Santa Clara, U.S.A.). Some drops of this bacterial culture were cast on sterilized glass and covered with a coverslip. Images of bacterial cells were acquired by using an inverted Zeiss microscope (Axiovert S100) with a 50× objective, equipped with a cooled DVC color camera. Transmission measurements were carried out by using a 100 W halogen lamp, whereas fluorescence measurements were acquired by using the green line (546 nm) of a 75 W Hg lamp as excitation source. By using an optical fiber (100 μm core size) positioned on the image plane equivalent to that of the camera, the spectral information was obtained on a defined portion of the image (1 μm sized). The extinction and fluorescence spectra were collected at various sites by using an array dual spectrometer (Avantes) as detecting device. The resolution of the extinction and fluorescence spectrum is 0.7 and 4 nm, respectively. The background absorbance and fluorescence values were collected outside the bacterial cells.

RESULTS AND DISCUSSION

Preparation and Morphology of PP-CD/TPPS Fabric.

PP nonwoven fabrics functionalized with HP-βCD (PP-CD) were fabricated as previously reported.[21] They consist of PP fibers coated by a cross-linked CD polymer issued from the polyesterification reaction between CTR and HP-βCD (polyCTR-CD) in a curing oven. TPPS-loaded PP-CD fabric was prepared by dipping PP-CD patches (1 cm × 1 cm) into porphyrin aqueous solutions. The gradual uptake of the porphyrin can be easily monitored in situ by fluorescence emission spectroscopy on patches dipped into porphyrin solution for different times (Figure S1). Since after 2 h only a negligible increase of porphyrin amount embedded into the PP-CD was found, this time has been selected to maximize the content of TPPS onto the fabric. Several cycles of washing and drying were necessary to eliminate PS physically adsorbed on fabric, and not specifically bound to polyCTR-CD coating. On the contrary, by dipping PP nonwoven patches uncoated with polyCTR-CD in TPPS solution, no embedding of porphyrin was detected. The leakage of the dye in water from our functionalized fabric was monitored spectrophotometrically by following the increase of the TPPS absorption band, when 1 cm × 1 cm samples were dipped in 3 mL of water directly in a cuvette. In about 3 h at 25 °C, ≈26% of dye was released in aqueous solution (Figure S2). At longer times porphyrin release in water remarkably slowed (vide infra). The amount of TPPS embedded into the PP-CD was determined by using the molar extinction coefficient at the Soret maximum (5.33×10^5 M^{-1} cm^{-1}), after complete release of the dye in water. This latter was obtained through immersion of fabric samples into an aqueous solution saturated with 1-AdaOH. This reagent displaces TPPS from fabric to solution, due to its higher affinity for CD cavity. It has been found that each 1 cm × 1 cm sample is able to load 0.022 (±0.0019) mg that corresponds to 0.0215 (±0.0018) μmol of TPPS. These ± SD values, which mainly can be ascribed to homogeneity of the PP treatment (the precision of weight gain is ≅±1.5% wt), suggests a good reproducibility of the entrapping process and following washing off of physically adsorbed PS. In this way, by taking into account the displacement of TPPS included in CD cavity from 1-AdaOH, and considering CD grafted on PP as pure solid species with activity unitary, a K_a between PP-CD and TPPS of approximately 1.3×10^5 M^{-1} was estimated. Although K_a was obtained by a simplified procedure (see Materials and Methods), it fairly agrees with the reported binding constant of βCD/1-AdaOH complex (≅9.8×10^4 M^{-1})[55] in aqueous solution, whereas it is higher with respect to binding constants which have been determined by Kano et al. for the complexation of β-CD with TPPS in aqueous solution (K_1 ≅ 1.7×10^4 M^{-1} and K_2 ≅ 2.3×10^3 M^{-1})[34] by considering a host/guest molar ratio of 2:1. By knowing that the CD total concentration grafted on fabric is ≅0.506 μmol × cm^2 and is higher than the loaded TPPS (≅0.0215 μM × cm^2), we assume that most of TPPS is complexed in CD grafted on PP. Conversely, the entrapment in PP-CD fabric of a cationic porphyrin (H_2T_4) was proved, but only a very low amount was detected (data not shown), confirming the role of grafted CD which more strongly interacts with TPPS with respect to H_2T_4.[34] Therefore, PP-CD/TPPS finished fabric was selected for further investigations. Figure 1 shows a schematic representation of the PP-CD/TPPS fabric preparation together

DOI: 10.1021/acs.biomac.6b01752
Biomacromolecules XXXX, XXX, XXX−XXX

with FEG-SEM and the corresponding optical micrographies. These latters evidence the entanglement of TPPS onto the fibers and, in particular, FEG-SEM reveals no prominent morphology modification, due to the chromophores inclusion, with respect to the PP-CD fibers precursor (Figure S3), except for a detectable increase of the fiber roughness.

Spectroscopic and Photophysical Studies. Spectroscopic characterization on PP-CD/TPPS fabric surface was carried out in order to elucidate the interaction sites of TPPS into the fibers and its photodynamic potential. Fluorescence emission spectra showed the typical two-banded emission profiles for this porphyrin with maxima centered at 654 and 715 nm, respectively (Figure 2). According to literature, these

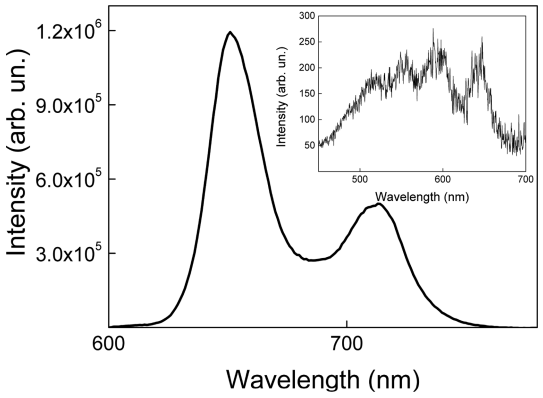

Figure 2. Fluorescence emission (λ_{exc} = 420 nm) and the corresponding excitation spectra (λ_{em} = 654 nm, inset) of PP-CD/TPPS fabric, at T = 25 °C.

features were attributed to TPPS entrapped in the CD-modified macromolecular matrix.[56] Moreover, the excitation profile in the Q-bands region shows the presence of four bands centered at 520, 554, 595, and 643 nm that match the Q-bands extinction spectra of PS, confirming the embedding of TPPS in the polyCTR-CD coating (Figure 2, inset).[56]

Since aggregation of porphyrins plays a key role in the photodynamic activity,[57] fluorescence lifetimes were measured to determine the PS aggregation state into the fabric. Time-resolved fluorescence measurements carried out at room temperature showed a biexponential decay with a short lifetime of 1.5 ns (37% amplitude), ascribable to oligomeric supramolecular aggregates and a long-living emitting species with lifetime of 8.3 ns (63% amplitude) due to porphyrin monomer (data not shown).[58] The presence of the monomeric species with longer lifetime guarantees a significant photodynamic inactivation. In order to ascertain the generation of $^1O_2$, species mainly responsible for photodamage, a phosphorescence profile of $^1O_2$ monitored by infrared luminescence at 1270 nm has been registered in air (Figure 3). The typical kinetic trace has been fitted by a first-order decay[52,59] with a lifetime (τ_Δ) of approximately 67 μs.

Even if the photophysical behavior of PP-CD/PS textile needs further studies, the lengthening of τ_Δ in TPPS-loaded fabric in air versus porphyrin immobilized inside nanofibers[8] agrees with PS accommodation on the surface of PP-CD. Furthermore, PP-CD/TPPS materials are hydrophilic and highly wettable, as demonstrated by sustained release in physiological media (vide infra). Therefore, our fabric, similar to other nanofibers externally modified with PS,[60] is promising to photodamage target species localized close to the surface.

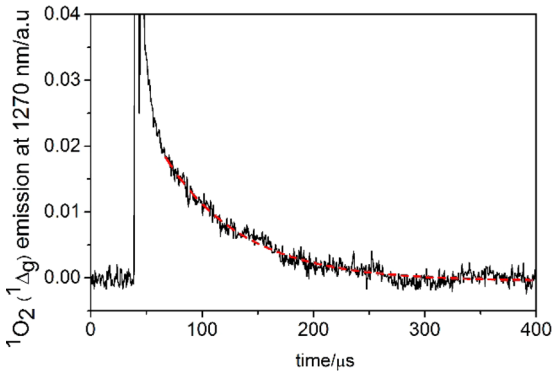

Figure 3. Typical kinetic trace of $^1O_2$ generated upon laser excitation (532 nm) of PP-CD/TPPS fabric (T = 25 °C) in air. The trace was best-fitted by first-order kinetic equation (red).

XPS and FTIR Characterization. XPS analysis was carried out in order to get insights on the complexation sites of TPPS in PP-CD. Analysis was performed by focusing selected small areas that resulted visually enriched (red area) or depleted (white area) by porphyrin. The S 2p photoelectron peak on the surface of PP-CD/TPPS was detected at a binding energy BE = 168.3 eV, and it is assigned to the presence of sulfonate groups.[61] The C 1s spectrum is dominated by the hydrocarbon component with a shallow tail in the high binding energy side. The curve-fitting procedure indicated the presence of several carbon species in different chemical environments, mainly due to N and O. Results of the XPS curve-fitting of the C 1s photoelectron peak in the white (A) and red (B) areas of a PP-CD/TPPS sample are shown in Figure 4. In Table 1, the surface distribution of carbon species, expressed as percentage of the total carbon peak area (100%), is reported. Both in the white and red areas of the sample, the C 1s signal can be deconvoluted by five components, corresponding to C−C/C−H, C−N, C−O, O−C−O, and O−C═O bonding states.[61] The presence of the oxygenated components in the 286−290 eV binding energy range resulted more evident in the C 1s spectrum of the red area (Figure 4B). As shown by the surface distribution of carbon species in Table 1, the intensity of all of the C−N and C−O components increased in the red area compared to the white area. This evidence can be attributed to the presence of the polyCTR-CD/TPPS coating on the PP fibers.

The FTIR analysis of the PP-CD/TPPS fabric is reported in Figure 5. FTIR spectra on the right side refer to the areas in the infrared chemical image (left) pointed by arrows.

The chemical images were obtained by measuring the intensity of the resonance at 1649 cm^{-1} attributed to O−C═O stretching of polyCTR-CD. Analysis of the intensities confirms that blue, green and red area in the chemical images are mostly occupied by PP fibers, PP-CD and PP-CD/TPPS, respectively. However, in all the areas, contributions due to polyCTR-CD/TPPS functionalization (in the range 1800−1500 cm^{-1}) can be evidenced. Figure 5A reports the FTIR spectrum in the area covered mostly by PP fibers.[62] In Figure 5B, signals in the 2900−3600 cm^{-1} range reflect contributions of primary and secondary OH groups of CD and of water located inside the CD cavity or at the interstices between different CD molecules.[63] In the 1800−1500 cm^{-1} region, the signals attributed to O−C═O stretching of the citrate linked to CD were observed. Also, in the same range, resonances ascribable to phenyl ring of TPPS appeared, even if they are less intense.[64]

DOI: 10.1021/acs.biomac.6b01752
Biomacromolecules XXXX, XXX, XXX−XXX

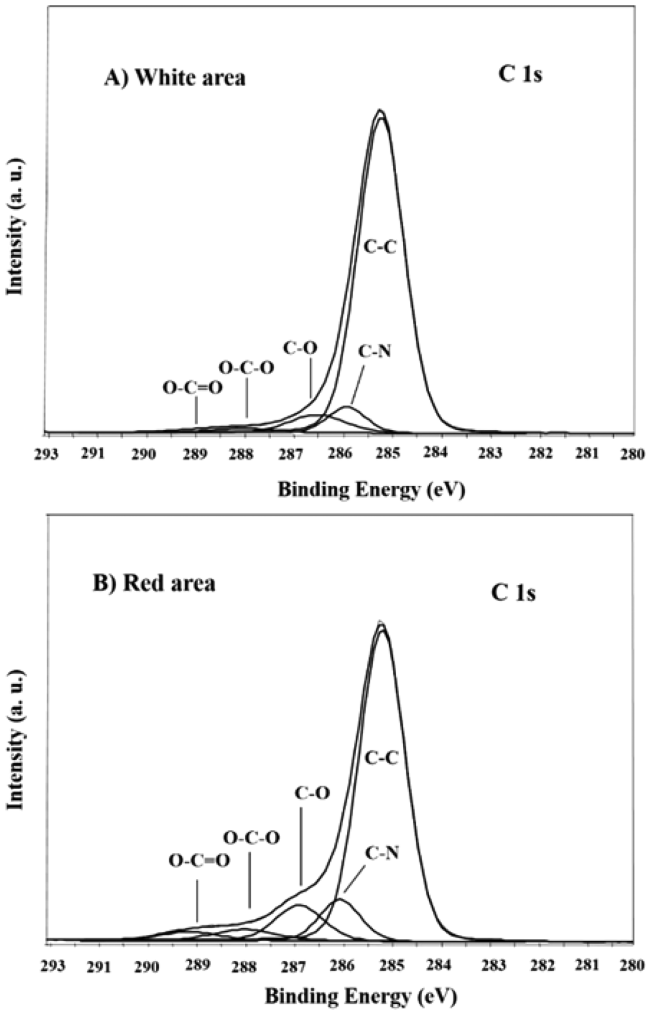

Figure 4. XPS curve-fitting of C 1s photoelectron peak in the white (A) and red (B) areas of the PP-CD/TPPS sample.

Table 1. XPS Surface Distribution of Carbon Species in the White and Red Areas of the PP-CD/TPPS Sample, Expressed As Percentage of the Total Carbon Peak Area (100%)

C 1s component	C−C	C−N	C−O	O−C−O	O−C═O
BE (eV)	285.1	285.9	286.6	287.8	288.9
A (white area)	86.0	5.9	5.9	1.6	0.6
B (red area)	75.9	8.8	8.9	3.7	2.7

These bands, pointed by black arrows in Figure 5B, remarkably changed in the red area corresponding to PP-CD/TPPS fabric (Figure 5C), thus, pointing out the interaction of TPPS with CTR moieties close to CD rims.

Release Kinetics and Competition Experiments. All the spectroscopic data indicated the successful entrapping of TPPS in cyclodextrin portions of the PP-CD matrix. Even if it is not possible, a priori to rule out an aspecific entanglement of TPPS on the PP sections of finished fabric, the interaction of TPPS with CD cavity was visually demonstrated by competition experiments in the presence of 1-Ada-OH (Figure S4). This latter, interacting preferentially with the CD cavity, displaces TPPS from fabric as evidenced by its rapid elution both in aqueous solutions (Figure 6) and in PBS (Figure S5) in comparison with the release in absence of 1-AdaOH. These results agree with the literature data demonstrating the inclusion of phenyl-sulfonate group of TPPS into the CD cavity.[34]

Furthermore, the release profiles of TPPS from PP-CD/TPPS were evaluated under physiological conditions. As reported in Figure 7, after a burst effect during the first hour with a release of about 50% of PS, the system is able to sustain TPPS release for about 2 days. The elution of TPPS from fabric in PBS was extremely slower at 25 °C than at 37 °C (Figure S6). This evidence points out to potential applications of this fabric as porphyrin eluting system in biologically relevant medium both close to room and physiological temperature.

Altogether, these results could bring out the feasibility to apply our textile device in controlling the amount of released PS, by changing time of exposure to infected biological sites and typology of CD-avid molecules. These latter could be uptaken from biological media and be contended with porphyrin for CD cavity or be externally coentrapped and released differently than PS.

Biological Investigations. Biological studies were, first, focused on *S. aureus*, a microorganism that showed to be sensitive to PDT by TPPS[65] and, in the second part, experiments were carried out also with *P. aeruginosa*, a microorganism not sensitive to TPPS treatment.[65]

TPPS Uptake and Antimicrobial Photodynamic Effect on *S. aureus*. As PS uptake seems to be related to photodynamic efficiency, uptake investigations have been performed.[66] A *S. aureus* suspension was incubated in the dark with PP-CD/TPPS fabric, washed to eliminate free TPPS, transferred onto glass and covered with coverslip (see Materials and Methods).

In Figure 8 are reported the transmission (A) and fluorescence optical images (C) of the cast bacterial suspension, respectively. UV−vis extinction spectra (Figure 8B) registered on bacterial cells show a band with a maximum at 420 nm, ascribed to TPPS. The presence of PS into the bacterial cells was confirmed by fluorescence emission spectra, which show the peculiar bands centered at 651 and 718 nm, respectively. Even if this setup needs some implementation for quantitative analysis of internalized PS, microscopic observations and spectral changes are in agreement with the uptake of TPPS into *S. aureus* cells and, in particular, within the cell wall[66] (high fluorescence in the peripheral regions in Figure 8C could be ascribed to insoluble fabric residues). The antibacterial efficacy of PP-CD/TPPS patch was investigated by a comparison of the number of viable cells in the *S. aureus* suspension incubated in the dark with fabric and irradiated, compared to that one incubated in the dark with patch and not irradiated. As a control, *S. aureus* was incubated with PP-CD and irradiated by confirming that, in the absence of PS, a light dose equal to that one here used (i.e., 5 J/cm^2) does not exert a substantial bactericidal effect.[67]

Viable cells collected from irradiated PP-CD/TPPS patches were 4 unit log lower than that collected from not irradiated patches, corresponding to 99.98% kill (cells from not irradiated patches were 4.3×10^6 versus 8×10^2 from irradiated ones, see Figure 9, left). Microscopic observation showed that, although single bacteria were not observable, a widespread green signal compatible with viable cells were linked to fibers of not irradiated patches (Figure 9A), whereas a low signal was observed in irradiated PP-CD/TTPS fabric(Figure 9B). More importantly, almost all the cells were red-stained after 30 min incubation with LIVE/DEAD. These data suggest that the cell

DOI: 10.1021/acs.biomac.6b01752
Biomacromolecules XXXX, XXX, XXX−XXX

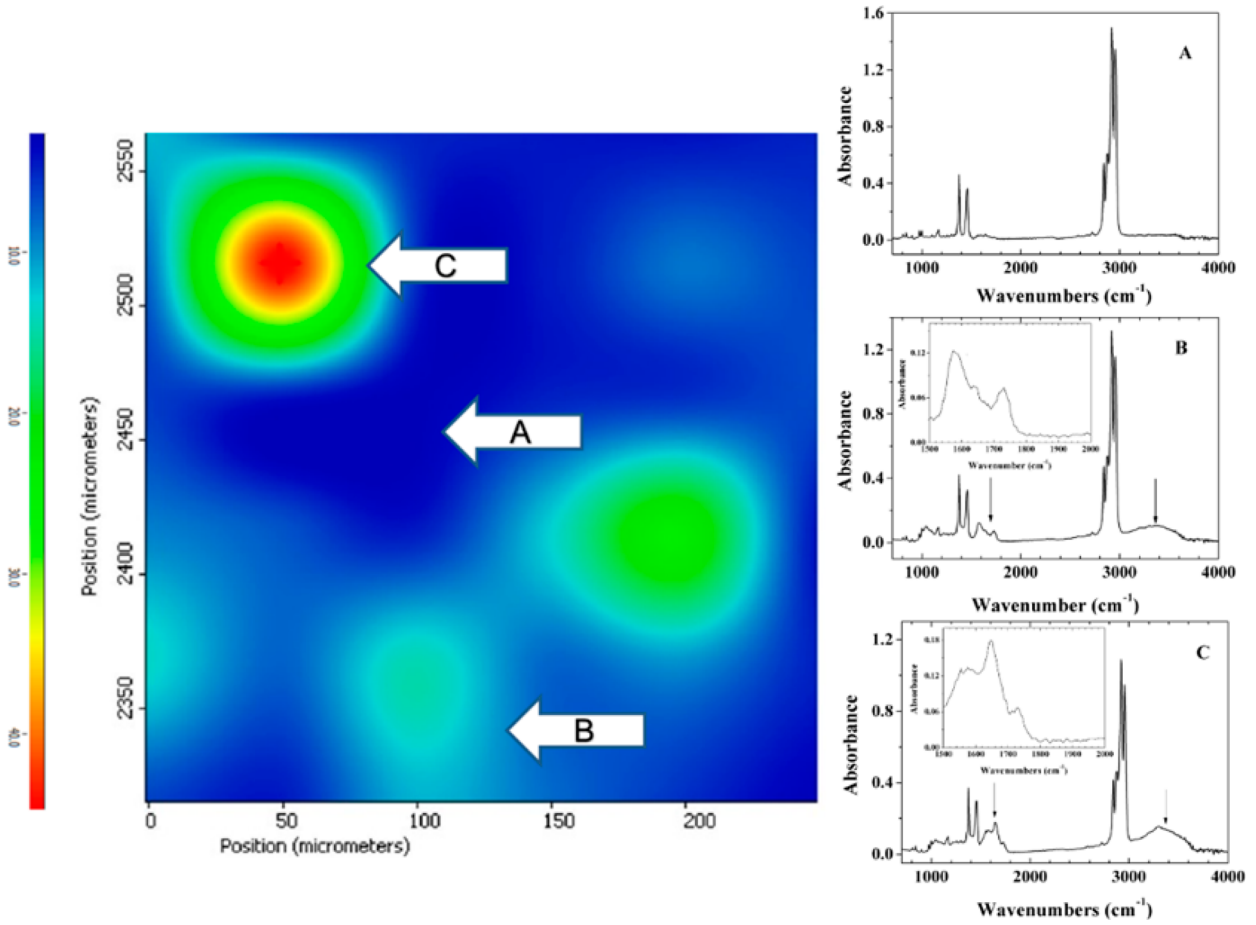

Figure 5. FTIR analysis of the PP-CD/TPPS fabric. FTIR spectra on the right refer to the corresponding areas in the infrared chemical image on the left pointed by the white arrows: A refers to the blue area (PP), B refers to the green area (PP-CD), and C refers to the red area (PP-CD/TPPS). Blue corresponds to zero intensity and red to the maximum intensity in the chromatic scale.

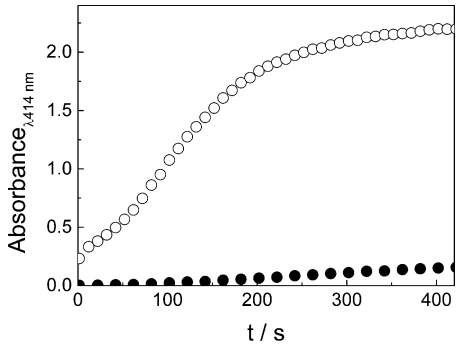

Figure 6. Elution profile of TPPS in aqueous solution (full circles) and in the presence of 1-AdaOH (empty circles) from PP-CD/TPPS (1 cm × 1 cm, T = 25 °C, SD ≤ 0.5%).

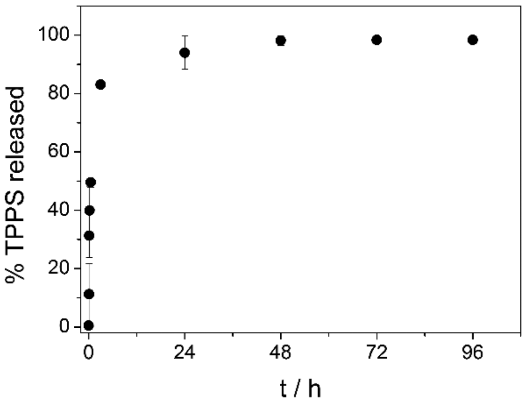

Figure 7. In vitro release profile of TPPS in PBS (10 mM, pH = 7.4 at 37 °C) from PP-CD/TPPS (1 cm × 1 cm). Data are reported as the mean of three independent experiments ± SD.

membranes of *S. aureus* were altered after patches irradiation, explaining the great decrease in the observed cell density.

Antimicrobial Photodynamic Effect on *P. aeruginosa*. Photodynamic antimicrobial activity of PP-CD/TPPS fabric was also investigated against *P. aeruginosa*, with the aim to increase the sensitivity of these Gram-negative bacteria toward TPPS with respect to the reported issues.[65] The rationale of this attempt relies with the achievement of uptake of this PS by exploiting, in principle, the help of CD that can sustain TPPS release. Differently from *S. aureus*, *P. aeruginosa* cultures incubated with PP-CD/TPPS fabric and irradiated did not undergo to valuable reduction (cells from not irradiated patches were 1.7×10^6 vs 1.8×10^6 from irradiated ones, see Figure 9, left). The microscopic observation (Figure 9C, D) also showed adhesion of *P. aeruginosa* cells, arranged on the fabric in both samples. In this case, the LIVE/DEAD staining showed fully viable bacteria (green color). These data, in agreement with literature, confirm that *P. aeruginosa* is much more tolerant to photodynamic action than other bacteria.[65]

DOI: 10.1021/acs.biomac.6b01752
Biomacromolecules XXXX, XXX, XXX−XXX

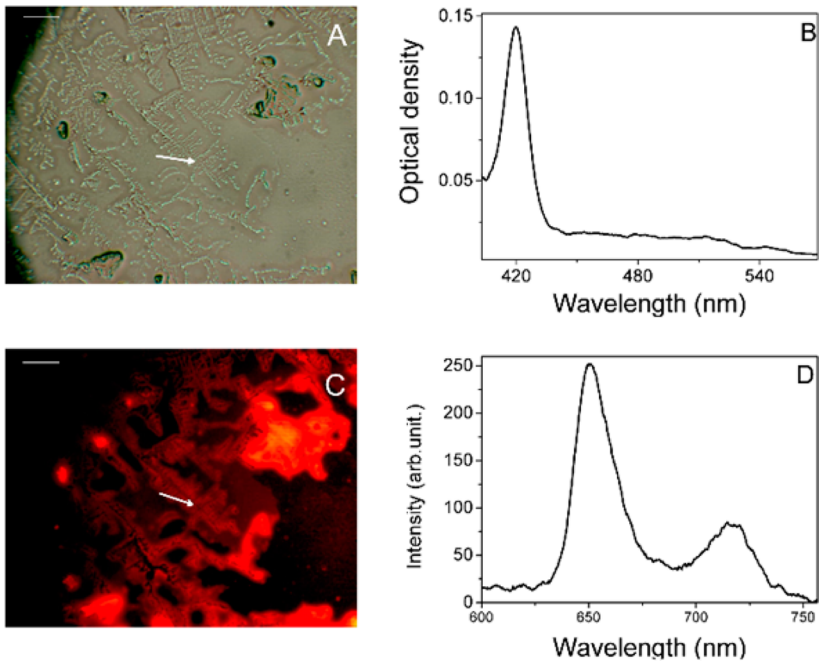

Figure 8. TPPS uptake studies: transmission (A) and fluorescence microscope images (C) with correspondent UV−vis extinction (B) and fluorescence emission spectra (D) on cells of *S. aureus*. Bacterial cells were incubated in the dark with PP-CD/TPPS, purified by free TPPS, and cast on glass. The bars in A and C are 20 μm. Spectra were acquired on the bacterial cells pointed by white arrows in the microscopy images.

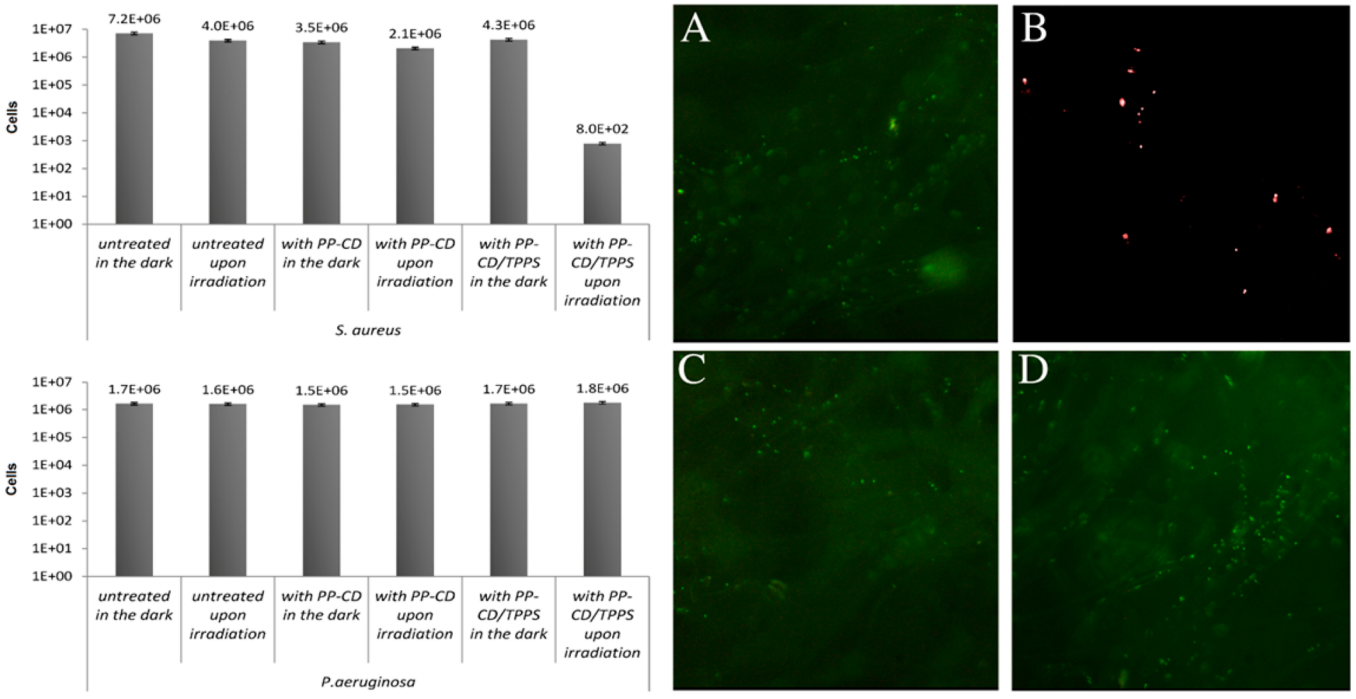

Figure 9. Photoantibacterial activity on *S. aureus* and *P. aeruginosa* incubated with PP-CD and PP-CD/TPPS fabric. Estimation of viable cells number (left) and corresponding visualization (right) by epifluorescence microscopy after staining with LIVE/DEAD (*S. aureus*: A and B; *P. aeruginosa*: C and D). The antibacterial efficacy and antiadhesive properties were evaluated before (A, C) and after irradiation (B, D).

A satisfying PDT activity by TPPS was observed against *S. aureus*. Considering a 50% of entrapped TPPS released in 30 min of incubation, a concentration ≅ 4 μM was released by fabric under the tested conditions. This amount of TPPS is reasonably lower with respect to free TPPS concentration utilized in solution to partially photoinactivate *S. aureus*, even if in that case the samples were irradiated with a lower dose of light (0.5 J/cm^2).[65] Although the solution of cationic PS (i.e., methylene blue and cationic porphyrins) is much more effective against bacteria, including *S. aureus*,[38,68] conversely the utilized amount of TPPS or other anionic PSs in solution are higher[65] or somewhere comparable to our results.[36,69]

Altogether, our findings suggests the feasibility of TPPS-loaded fabric to concentrate and release anionic PS in physiological medium to photoinactivate *S. aureus*. This approach could be promising to design implants with

DOI: 10.1021/acs.biomac.6b01752
Biomacromolecules XXXX, XXX, XXX−XXX

photodynamic properties, which can be activated by optical fiber using light at suitable wavelengths in the postsurgical treatment of local infections, minimizing the systemic exposure of PS solutions and nanoparticles dispersions.[44]

CONCLUSIONS

Fabric based on polypropylene nonwoven fibers coated with citric acid-hydroxypropyl-βCD crosslinked polymer and loaded with an anionic porphyrin were designed and fully characterized by complementary spectroscopic and microscopic techniques. Our findings pointed out that porphyrin is hosted into the CD cavity, presumably by exploiting the interactions both with inner and CTR-conjugate rims of macrocycle. These fabrics are able to elute about 50% photosensitizer in few hours and sustain its release in physiologic conditions for about 3 days. Together with their propensity to photoinactivate *S. aureus*, these properties strongly support further research on textile-based photosensitizer eluting system for potential aPDT applications as coverings or implants in infected sites. Both the control of the released photosensitizer versus time of exposure of fabric to the infection and the codelivery of other cyclodextrin avid drugs, open the way to investigate novel multifunctional textiles against multidrug-resistant bacteria.

ASSOCIATED CONTENT

Supporting Information

The Supporting Information is available free of charge on the ACS Publications website at DOI: 10.1021/acs.biomac.6b01752.

Fluorescence emission spectra of samples at different dipping times in PS aqueous solutions (Figure S1); Elution profile of TPPS from fabric in aqueous solution (Figure S2); FEG-SEM images of PP-CD precursor and PP-CD/TPPS (Figure S3); Pictures of PP-CD/TPPS after dipping in aqueous solution and in the presence of a saturated aqueous solution of 1-AdaOH (Figure S4); Release profiles of TPPS in PBS and in PBS enriched with 1-AdaOH (Figure S5); Release profiles of TPPS in PBS from PP-CD/TPPS fabric at different temperatures (Figure S6) (PDF).

AUTHOR INFORMATION

Corresponding Author

*Tel./Fax: +39 090 3974108. E-mail: antonino.mazzaglia@ismn.cnr.it.

ORCID

Maria Angela Castriciano: 0000-0002-1514-8820

Valentina Villari: 0000-0002-7907-842X

Antonino Mazzaglia: 0000-0002-3140-5655

Author Contributions

The manuscript was written through contributions of all authors. All authors have given approval to the final version of the manuscript.

Notes

The authors declare no competing financial interest.

ACKNOWLEDGMENTS

XPS technical support by Dr. Andrew Wright, ThermoFischer Scientific, Surface Analysis, East Grinstead, U.K., and FTIR technical support by Dr. Massimiliano Rocchia, Thermo Fisher Scientific, Rodano (Mi), Italy, are gratefully acknowledged. Support from Prof. Salvatore Sortino (University of Catania) for singlet oxygen detection and from Dr. Gabriel Maria Ingo (CNR-ISMN, Montelibretti) for microscopy facilities was strongly appreciated. The authors thank MIUR (PRIN 2010-2011 Project No. 2010C4RM8) and CNR for financial support.

REFERENCES

(1) *Nanobiomaterials in Antimicrobial Therapy: Applications of Nanobiomaterials*; Elsevier: Cambridge, U.S.A., 2016.

(2) Dai, T.; Huang, Y.-Y.; Hamblin, M. R. Photodynamic Therapy for Localized Infections—State of the Art. *Photodiagn. Photodyn. Ther.* **2009**, *6*, 170−188.

(3) Hamblin, M. R.; Hasan, T. Photodynamic Therapy: A New Antimicrobial Approach to Infectious Disease? *Photochem. Photobiol. Sci.* **2004**, *3*, 436−450.

(4) Jiang, L.; Gan, C. R. R.; Gao, J.; Loh, X. J. A Perspective on the Trends and Challenges Facing Porphyrin-Based Anti-Microbial Materials. *Small* **2016**, *12*, 3609−3644.

(5) Craig, R. A.; McCoy, C. P.; Gorman, S. P.; Jones, D. S. Photosensitisers − the Progression from Photodynamic Therapy to Anti-Infective Surfaces. *Expert Opin. Drug Delivery* **2015**, *12*, 85−101.

(6) McCoy, C. P.; Craig, R. A.; McGlinchey, S. M.; Carson, L.; Jones, D. S.; Gorman, S. P. Surface Localisation of Photosensitisers on Intraocular Lens Biomaterials for Prevention of Infectious Endophthalmitis and Retinal Protection. *Biomaterials* **2012**, *33*, 7952−7958.

(7) Henke, P.; Kozak, H.; Artemenko, A.; Kubát, P.; Forstová, J.; Mosinger, J. Superhydrophilic Polystyrene Nanofiber Materials Generating $O_2(^1\Delta_g)$: Postprocessing Surface Modifications toward Efficient Antibacterial Effect. *ACS Appl. Mater. Interfaces* **2014**, *6*, 13007−13014.

(8) Mosinger, J.; Jirsak, O.; Kubat, P.; Lang, K.; Mosinger, B. Bactericidal Nanofabrics Based on Photoproduction of Singlet Oxygen. *J. Mater. Chem.* **2007**, *17*, 164−166.

(9) Arenbergerova, M.; Arenberger, P.; Bednar, M.; Kubat, P.; Mosinger, J. Light-Activated Nanofibre Textiles Exert Antibacterial Effects in the Setting of Chronic Wound Healing. *Exp Dermatol* **2012**, *21*, 619−624.

(10) Lhotakova, Y.; Plistil, L.; Moravkova, A.; Kubat, P.; Lang, K.; Forstova, J.; Mosinger, J., Virucidal Nanofiber Textiles Based on Photosensitized Production of Singlet Oxygen. *PLoS One* **2012**, 7.e4922610.1371/journal.pone.0049226

(11) Redl, F. X.; Lutz, M.; Daub, J. Chemistry of Porphyrin-Appended Cellulose Strands with a Helical Structure: Spectroscopy, Electrochemistry, and in Situ Circular Dichroism Spectroelectrochemistry. *Chem. - Eur. J.* **2001**, *7*, 5350−5358.

(12) Carpenter, B. L.; Scholle, F.; Sadeghifar, H.; Francis, A. J.; Boltersdorf, J.; Weare, W. W.; Argyropoulos, D. S.; Maggard, P. A.; Ghiladi, R. A. Synthesis, Characterization, and Antimicrobial Efficacy of Photomicrobicidal Cellulose Paper. *Biomacromolecules* **2015**, *16*, 2482−2492.

(13) Hsu, B. B.; Klibanov, A. M. Light-Activated Covalent Coating of Cotton with Bactericidal Hydrophobic Polycations. *Biomacromolecules* **2011**, *12*, 6−9.

(14) Krouit, M.; Granet, R.; Krausz, P. Photobactericidal Films from Porphyrins Grafted to Alkylated Cellulose − Synthesis and Bactericidal Properties. *Eur. Polym. J.* **2009**, *45*, 1250−1259.

(15) Dastjerdi, R.; Montazer, M. A Review on the Application of Inorganic Nano-Structured Materials in the Modification of Textiles: Focus on Anti-Microbial Properties. *Colloids Surf., B* **2010**, *79*, 5−18.

(16) Khantamat, O.; Li, C.-H.; Yu, F.; Jamison, A. C.; Shih, W.-C.; Cai, C.; Lee, T. R. Gold Nanoshell-Decorated Silicone Surfaces for the near-Infrared (Nir) Photothermal Destruction of the Pathogenic Bacterium E. Faecalis. *ACS Appl. Mater. Interfaces* **2015**, *7*, 3981−3993.

(17) Millenbaugh, N. J.; Baskin, J. B.; DeSilva, M. N.; Elliott, W. R.; Glickman, R. D. Photothermal Killing of Staphylococcus Aureus Using Antibody-Targeted Gold Nanoparticles. *Int. J. Nanomed.* **2015**, *10*, 1953−1960.

DOI: 10.1021/acs.biomac.6b01752
Biomacromolecules XXXX, XXX, XXX−XXX

(18) Sobocinski, J.; Laure, W.; Taha, M.; Courcot, E.; Chai, F.; Simon, N.; Addad, A.; Martel, B.; Haulon, S.; Woisel, P.; Blanchemain, N.; Lyskawa, J. Mussel Inspired Coating of a Biocompatible Cyclodextrin Based Polymer onto CoCr Vascular Stents. *ACS Appl. Mater. Interfaces* **2014**, *6*, 3575−3586.
(19) Blanchemain, N.; Karrout, Y.; Tabary, N.; Neut, C.; Bria, M.; Siepmann, J.; Hildebrand, H. F.; Martel, B. Methyl-B-Cyclodextrin Modified Vascular Prosthesis: Influence of the Modification Level on the Drug Delivery Properties in Different Media. *Acta Biomater.* **2011**, *7*, 304−314.
(20) El Ghoul, Y.; Blanchemain, N.; Laurent, T.; Campagne, C.; El Achari, A.; Roudesli, S.; Morcellet, M.; Martel, B.; Hildebrand, H. F. Chemical, Biological and Microbiological Evaluation of Cyclodextrin Finished Polyamide Inguinal Meshes. *Acta Biomater.* **2008**, *4*, 1392−1400.
(21) Laurent, T.; Kacem, I.; Blanchemain, N.; Cazaux, F.; Neut, C.; Hildebrand, H. F.; Martel, B. Cyclodextrin and Maltodextrin Finishing of a Polypropylene Abdominal Wall Implant for the Prolonged Delivery of Ciprofloxacin. *Acta Biomater.* **2011**, *7*, 3141−3149.
(22) Lichter, J. A.; Van Vliet, K. J.; Rubner, M. F. Design of Antibacterial Surfaces and Interfaces: Polyelectrolyte Multilayers as a Multifunctional Platform. *Macromolecules* **2009**, *42*, 8573−8586.
(23) Séon, L.; Lavalle, P.; Schaaf, P.; Boulmedais, F. Polyelectrolyte Multilayers: A Versatile Tool for Preparing Antimicrobial Coatings. *Langmuir* **2015**, *31*, 12856−12872.
(24) Lewis, K.; Klibanov, A. M. Surpassing Nature: Rational Design of Sterile-Surface Materials. *Trends Biotechnol.* **2005**, *23*, 343−348.
(25) Decher, G.; Hong, J. D.; Schmitt, J. Buildup of Ultrathin Multilayer Films by a Self-Assembly Process: III. Consecutively Alternating Adsorption of Anionic and Cationic Polyelectrolytes on Charged Surfaces. *Thin Solid Films* **1992**, *210−211* (Part 2), 831−835.
(26) Junthip, J.; Tabary, N.; Leclercq, L.; Martel, B. Cationic B-Cyclodextrin Polymer Applied to a Dual Cyclodextrin Polyelectrolyte Multilayer System. *Carbohydr. Polym.* **2015**, *126*, 156−167.
(27) Junthip, J.; Tabary, N.; Chai, F.; Leclercq, L.; Maton, M.; Cazaux, F.; Neut, C.; Paccou, L.; Guinet, Y.; Staelens, J.-N.; Bria, M.; Landy, D.; Hédoux, A.; Blanchemain, N.; Martel, B. Layer-by-Layer Coating of Textile with Two Oppositely Charged Cyclodextrin Polyelectrolytes for Extended Drug Delivery. *J. Biomed. Mater. Res., Part A* **2016**, *104*, 1408−1424.
(28) Nazi, M.; Malek, R. M. A.; Kotek, R. Modification of Beta-Cyclodextrin with Itaconic Acid and Application of the New Derivative to Cotton Fabrics. *Carbohydr. Polym.* **2012**, *88*, 950−958.
(29) Hebeish, A.; El-Sawy, S. M.; Ragaei, M.; Hamdy, I. A.; El-Bisi, M. K.; Abdel-Mohdy, F. A. New Textiles of Biocidal Activity by Introduce Insecticide in Cotton-Poly (GMA) Copolymer Containing *β*-Cd. *Carbohydr. Polym.* **2014**, *99*, 208−217.
(30) Issazadeh- Baltorki, H.; Khoddami, A. Cyclodextrin-Coated Denim Fabrics as Novel Carriers for Ingredient Deliveries to the Skin. *Carbohydr. Polym.* **2014**, *110*, 513−517.
(31) Martin, A.; Tabary, N.; Chai, F.; Leclercq, L.; Junthip, J.; Aubert-Viard, F.; Neut, C.; Weltrowski, M.; Nicolas, B.; Bernard, M. Build-up of an Antimicrobial Multilayer Coating on a Textile Support Based on a Methylene Blue−Poly(Cyclodextrin) Complex. *Biomed. Mater.* **2013**, *8*, 065006.
(32) Kettel, M. J.; Schaefer, K.; Groll, J.; Moeller, M. Nanogels with High Active *β*-Cyclodextrin Content as Physical Coating System with Sustained Release Properties. *ACS Appl. Mater. Interfaces* **2014**, *6*, 2300−2311.
(33) Mazzaglia, A., Cyclodextrins in Pharmaceutics, *Cosmetics, and Biomedicine Current and Future Industrial Applications*; John Wiley and Sons, 2015; Vol. *135*, pp 343−351.
(34) Kano, K.; Nishiyabu, R.; Asada, T.; Kuroda, Y. Static and Dynamic Behavior of 2:1 Inclusion Complexes of Cyclodextrins and Charged Porphyrins in Aqueous Organic Media. *J. Am. Chem. Soc.* **2002**, *124*, 9937−9944.
(35) Banfi, S.; Caruso, E.; Buccafurni, L.; Battini, V.; Zazzaron, S.; Barbieri, P.; Orlandi, V. Antibacterial Activity of Tetraaryl-Porphyrin Photosensitizers: An in Vitro Study on Gram Negative and Gram Positive Bacteria. *J. Photochem. Photobiol., B* **2006**, *85*, 28−38.
(36) Tomé, J. P. C.; Neves, M. G. P. M. S.; Tomé, A. C.; Cavaleiro, J. A. S.; Soncin, M.; Magaraggia, M.; Ferro, S.; Jori, G. Synthesis and Antibacterial Activity of New Poly-S-Lysine−Porphyrin Conjugates. *J. Med. Chem.* **2004**, *47*, 6649−6652.
(37) Alves, E.; Costa, L.; Carvalho, C. M.; Tomé, J. P.; Faustino, M. A.; Neves, M. G.; Tomé, A. C.; Cavaleiro, J. A.; Cunha, Â.; Almeida, A. Charge Effect on the Photoinactivation of Gram-Negative and Gram-Positive Bacteria by Cationic Meso-Substituted Porphyrins. *BMC Microbiol.* **2009**, *9*, 70.
(38) Demidova, T. N.; Hamblin, M. R. Photodynamic Therapy Targeted to Pathogens. *Int. J. Immunopathol. Pharmacol.* **2004**, *17*, 245−254.
(39) Ferro, S.; Jori, G.; Sortino, S.; Stancanelli, R.; Nikolov, P.; Tognon, G.; Ricchelli, F.; Mazzaglia, A. Inclusion of 5-[4-(1-Dodecanoylpyridinium)]-10,15,20-Triphenylporphine in Supramolecular Aggregates of Cationic Amphiphilic Cyclodextrins: Physicochemical Characterization of the Complexes and Strengthening of the Antimicrobial Photosensitizing Activity. *Biomacromolecules* **2009**, *10*, 2592−2600.
(40) Wainwright, M. Photodynamic Antimicrobial Chemotherapy (Pact). *J. Antimicrob. Chemother.* **1998**, *42*, 13−28.
(41) Tardivo, J. P.; Del Giglio, A.; de Oliveira, C. S.; Gabrielli, D. S.; Junqueira, H. C.; Tada, D. B.; Severino, D.; de Fátima Turchiello, R.; Baptista, M. S. Methylene Blue in Photodynamic Therapy: From Basic Mechanisms to Clinical Applications. *Photodiagn. Photodyn. Ther.* **2005**, *2*, 175−191.
(42) Zoltan, T.; Vargas, F.; López, V.; Chávez, V.; Rivas, C.; Ramírez, Á. H. Influence of Charge and Metal Coordination of Meso-Substituted Porphyrins on Bacterial Photoinactivation. *Spectrochim. Acta, Part A* **2015**, *135*, 747−756.
(43) Wilson, M. Light-Activated Antimicrobial Coating for the Continuous Disinfection of Surfaces. *Infect Control Hosp Epidemiol* **2003**, *24*, 782−784.
(44) Wainwright, M. Photodynamic Medicine and Infection Control. *J. Antimicrob. Chemother.* **2012**, *67*, 787−788.
(45) Di Poto, A.; Sbarra, M. S.; Provenza, G.; Visai, L.; Speziale, P. The Effect of Photodynamic Treatment Combined with Antibiotic Action or Host Defence Mechanisms on Staphylococcus Aureus Biofilms. *Biomaterials* **2009**, *30*, 3158−3166.
(46) Fu, X.-j.; Fang, Y.; Yao, M. Antimicrobial Photodynamic Therapy for Methicillin-Resistant Staphylococcus Aureus Infection. *BioMed Res. Int.* **2013**, *2013*, 9.
(47) Obritsch, M. D.; Fish, D. N.; MacLaren, R.; Jung, R. Nosocomial Infections Due to Multidrug-Resistant Pseudomonas Aeruginosa: Epidemiology and Treatment Options. *Pharmacother* **2005**, *25*, 1353−1364.
(48) Martel, B.; Ruffin, D.; Weltrowski, M.; Lekchiri, Y.; Morcellet, M. Water-Soluble Polymers and Gels from the Polycondensation between Cyclodextrins and Poly(carboxylic acid)s: A Study of the Preparation Parameters. *J. Appl. Polym. Sci.* **2005**, *97*, 433−442.
(49) Herbois, R.; Noël, S.; Léger, B.; Tilloy, S.; Menuel, S.; Addad, A.; Martel, B.; Ponchel, A.; Monflier, E. Ruthenium-containing *β*-Cyclodextrin Polymer Globules as Water-Compatible Microreactors for the Catalytic Hydrogenation of Biomass-derived Furanic Compounds. *Green Chem.* **2015**, *17*, 2444−2454.
(50) Fleischer, E. B.; Palmer, J. M.; Srivastava, T. S.; Chatterjee, A. Thermodyamic and Kinetic Properties of an Iron-Porphyrin System. *J. Am. Chem. Soc.* **1971**, *93*, 3162−3167.
(51) Iannazzo, D.; Mazzaglia, A.; Scala, A.; Pistone, A.; Galvagno, S.; Lanza, M.; Riccucci, C.; Ingo, G. M.; Colao, I.; Sciortino, M. T.; Valle, F.; Piperno, A.; Grassi, G. *β*-Cyclodextrin-Grafted on Multiwalled Carbon Nanotubes as Versatile Nanoplatform for Entrapment of Guanine-Based Drugs. *Colloids Surf., B* **2014**, *123*, 264−270.
(52) Kandoth, N.; Vittorino, E.; Sciortino, M. T.; Parisi, T.; Colao, I.; Mazzaglia, A.; Sortino, S.; Cyclodextrin-Based, A. Nanoassembly with Bimodal Photodynamic Action. *Chem. - Eur. J.* **2012**, *18*, 1684−1690.

DOI: 10.1021/acs.biomac.6b01752
Biomacromolecules XXXX, XXX, XXX−XXX

(53) Valli, L.; Giancane, G.; Mazzaglia, A.; Scolaro, L. M.; Conoci, S.; Sortino, S. Photoresponsive Multilayer Films by Assembling Cationic Amphiphilic Cyclodextrins and Anionic Porphyrins at the Air/Water Interface. *J. Mater. Chem.* **2007**, *17*, 1660−1663.
(54) Sherwood, P. M. A.; Briggs, D.; Seah, M. P. *Practical Surface Analysis*; Wiley: New York, 1990.
(55) Soto Tellini, V. H.; Jover, A.; García, J. C.; Galantini, L.; Meijide, F.; Tato, J. V. Thermodynamics of Formation of Host−Guest Supramolecular Polymers. *J. Am. Chem. Soc.* **2006**, *128*, 5728−5734.
(56) Mazzaglia, A.; Valerio, A.; Micali, N.; Villari, V.; Quaglia, F.; Castriciano, M. A.; Scolaro, L. M.; Giuffre, M.; Siracusano, G.; Sciortino, M. T. Effective Cell Uptake of Nanoassemblies of a Fluorescent Amphiphilic Cyclodextrin and an Anionic Porphyrin. *Chem. Commun.* **2011**, *47*, 9140−9142.
(57) Sortino, S.; Mazzaglia, A.; Monsù Scolaro, L.; Marino Merlo, F.; Valveri, V.; Sciortino, M. T. Nanoparticles of Cationic Amphiphilic Cyclodextrins Entangling Anionic Porphyrins as Carrier-Sensitizer System in Photodynamic Cancer Therapy. *Biomaterials* **2006**, *27*, 4256−4265.
(58) Castriciano, M. A.; Romeo, A.; Villari, V.; Angelini, N.; Micali, N.; Scolaro, L. M. Aggregation Behavior of Tetrakis(4-Sulfonatophenyl)Porphyrin in Aot/Water/Decane Microemulsions. *J. Phys. Chem. B* **2005**, *109*, 12086−12092.
(59) Mosinger, J.; Lang, K.; Plíštil, L.; Jesenská, S.; Hostomský, J.; Zelinger, Z.; Kubát, P. Fluorescent Polyurethane Nanofabrics: A Source of Singlet Oxygen and Oxygen Sensing. *Langmuir* **2010**, *26*, 10050−10056.
(60) Henke, P.; Lang, K.; Kubát, P.; Sýkora, J.; Šlouf, M.; Mosinger, J. Polystyrene Nanofiber Materials Modified with an Externally Bound Porphyrin Photosensitizer. *ACS Appl. Mater. Interfaces* **2013**, *5*, 3776−3783.
(61) Moulder, J. F.; Stickle, W. F.; Sobol, P. E.; Bomben, K. D. *Handbook of X-Ray Photoelectron Spectroscopy*; Eden Prairie, 1995.
(62) Morent, R.; De Geyter, N.; Leys, C.; Gengembre, L.; Payen, E. Comparison between XPS and FTIR-Analysis of Plasma-Treated Polypropylene Film Surfaces. *Surf. Interface Anal.* **2008**, *40*, 597−600.
(63) Cannava, C.; Stancanelli, R.; Marabeti, M. R.; Venuti, V.; Cascio, C.; Guarneri, P.; Bongiorno, C.; Sortino, G.; Majolino, D.; Mazzaglia, A.; Tommasini, S.; Ventura, C. A. Nanospheres Based on PLGA/Amphiphilic Cyclodextrin Assemblies as Potential Enhancers of Methylene Blue Neuroprotective Effect. *RSC Adv.* **2016**, *6*, 16720−16729.
(64) Zhang, Y.-H.; Chen, D.-M.; He, T.; Liu, F.-C. Raman and Infrared Spectral Study of Meso-Sulfonatophenyl Substituted Porphyrins ($TPPS_n$, n = 1, 2A, 2O, 3, 4). *Spectrochim. Acta, Part A* **2003**, *59*, 87−101.
(65) Hanakova, A.; Bogdanova, K.; Tomankova, K.; Binder, S.; Bajgar, R.; Langova, K.; Kolar, M.; Mosinger, J.; Kolarova, H. Study of Photodynamic Effects on NIH 3T3 Cell Line and Bacteria. *Biomed. Pap.* **2014**, *158*, 201−207.
(66) Mineo, P.; Faggio, C.; Micali, N.; Scamporrino, E.; Villari, V.; Star, A. Polymer Based on a Polyethylene Glycol with a Porphyrinic Core as a Photosensitizing Agent for Application in Photodynamic Therapy: Tests in Vitro on Human Erythrocytes. *RSC Adv.* **2014**, *4*, 19389−19395.
(67) Maclean, M.; MacGregor, S. J.; Anderson, J. G.; Woolsey, G. A. The Role of Oxygen in the Visible-Light Inactivation of Staphylococcus Aureus. *J. Photochem. Photobiol., B* **2008**, *92*, 180−184.
(68) Wainwright, M.; Phoenix, D. A.; Laycock, S. L.; Wareing, D. R. A.; Wright, P. A. Photobactericidal Activity of Phenothiazinium Dyes against Methicillin-Resistant Strains of Staphylococcus Aureus. *FEMS Microbiol. Lett.* **1998**, *160*, 177−181.
(69) Griffiths, M. A.; Wren, B. W.; Wilson, M. Killing of Methicillin-Resistant Staphylococcus Aureus in Vitro Using Aluminium Disulphonated Phthalocyanine, a Light-Activated Antimicrobial Agent. *J. Antimicrob. Chemother.* **1997**, *40*, 873−876.

DOI: 10.1021/acs.biomac.6b01752
Biomacromolecules XXXX, XXX, XXX−XXX